

Magic Islands and Barriers to Attachment: A Si/Si(111)7×7 Growth Model

J. Mysliveček* and T. Jarolímek

Department of Electronics and Vacuum Physics, Faculty of Mathematics and Physics, Charles University, V Holešovičkách 2, 180 00 Praha 8, Czech Republic

P. Šmilauer

Institute of Physics, Academy of Sciences of the Czech Republic, Cukrovarnická 10, 162 53 Praha 6, Czech Republic

B. Voigtländer and M. Kästner

Institut für Grenzflächenforschung und Vakuumphysik, Forschungszentrum Jülich, 52425 Jülich, Germany

(May 21, 2021)

Surface reconstructions can drastically modify growth kinetics during initial stages of epitaxial growth as well as during the process of surface equilibration after termination of growth. We investigate the effect of activation barriers hindering attachment of material to existing islands on the density and size distribution of islands in a model of homoepitaxial growth on Si(111)7×7 reconstructed surface. An unusual distribution of island sizes peaked around “magic” sizes and a steep dependence of the island density on the growth rate are observed. “Magic” islands (of a different shape as compared to those obtained during growth) are observed also during surface equilibration.

81.15.Aa, 05.70.Ln, 81.15.Hi, 68.35.Bs

Investigation of island structures formed during the initial stages of epitaxial growth allows us to explore kinetic mechanisms that govern the ordering of deposited atoms.¹ A lot of attention has recently focused on the time- and growth-conditions dependence of the island density² as well as on the bell-shaped distribution of island sizes² whose origin can be traced back to the distribution of island capture zones.³ However, real growth systems are invariably more complicated than the idealized models of epitaxy commonly used. For example, the presence of surface reconstructions can completely change the growth behavior.

In homoepitaxy of Si on Si(111)7×7 reconstructed surface, a process of “reconstruction destruction” was described by Tochihara and Shimada.⁴ The need to cancel surface reconstruction around a growing island gives rise to *barriers to attachment* of new material to existing islands. Growth with barriers to attachment has been already studied theoretically: The dependence of the island density on growth conditions was explored using analytic methods,^{5,6} while kinetic Monte Carlo (KMC) simulations of a simple growth model revealed an island size distribution multiple-peaked around “magic” sizes.⁷

Here we present a detailed KMC model of Si/Si(111)7×7 molecular beam epitaxy (MBE), with barriers to attachment included. With the help of this model we investigate the time- and growth-rate dependence of the island density, the shape of the island-size distribution, as well as island decay and filling of vacancy islands on the surface. The results of our simulations compare favorably to available experimental data about the Si/Si(111)7×7 system. We also discuss those features of the model kinetics that are specific to growth with barriers to attachment.

Dynamics of Si/Si(111)7×7 MBE growth was experi-

mentally studied by Voigtländer *et al.*^{8–10} The most interesting feature observed, the existence of kinetically stabilized magic sizes in the island size distribution, was reported and KMC modeled in Ref. 7. The model discussed in this work is a generalization of the model from Ref. 7 which is in turn based on the “reconstruction destruction” model of Si/Si(111)7×7 growth proposed by Tochihara and Shimada.⁴ The material is deposited in units (cf. below) that are randomly placed onto sites of a honeycomb lattice. These sites represent half-unit cells (HUCs) of Si(111)7×7 surface reconstruction. Two types of HUCs exist: In unfaulted HUCs (marked U), a surface atom bilayer follows bulk bilayer stacking, in faulted HUCs (marked F), the surface bilayer is 30° rotated with respect to the bulk, forming a stacking fault.¹¹ Material in a HUC may be either non-transformed (marked X, models the free Si adatoms diffusing on the reconstructed Si surface) or transformed (marked T, corresponds to a HUC, where the material underwent the reconstruction destruction process and subsequent crystallization). The model thus becomes *de facto* a two-species one. The non-transformed units of the material randomly walk on the surface, meet each other and transform. Transformation is an activated process, activation energy for transformation is supposed to be higher in F HUCs due to the need to remove the stacking fault.⁴

In the experiment, deposited material does not diffuse as HUCs.¹² The use of units of deposited material allows us to model easily collective processes during “reconstruction destruction” around island edges. Since, in general, the processes at island edges determine behavior of growth models (as they determine growth behavior of real systems), the simplification of material deposition and surface diffusion should not affect the model behavior in a substantial way. Our simulation scheme

is coarse-grained and ignores all processes on the length scales smaller than a HUC and on the time scales shorter than the time required to transport material from one HUC to its nearest neighbor.

The hopping rate for a HUC hop is $\nu_D = \nu_0 \exp(-E_D/k_B T)$ where $E_D = E_S + (x + t)E_N^X$ for an X-HUC, $E_D = E_S + xE_N^X + tE_N^T$ for a T-HUC, x and t being the numbers of X and T neighbors, respectively, E_N^X bond strengths of $X - X$ and $X - T$ pairs, E_N^T bond strength of a $T - T$ pair, and E_S the surface barrier to diffusion. The rate of an X-HUC transformation is $\nu_T = \nu_0 \exp(-E_T/k_B T)$ where $E_T^F = E_A - tE_{\text{edge}}$ for an F-HUC, $E_T^U = E_A - tE_{\text{edge}} - E_{\text{diff}}$ for a U-HUC, E_A being the barrier to attachment, E_{edge} a decrease in the barrier due to a transformed neighbor, and E_{diff} the barrier difference for F- and U-HUC overgrowth. Transformation of an island begins at an F-HUC with ≥ 2 X-neighbors, and the rate of this nucleation process is $\nu = \nu_0 \exp[(E_T - E_{\text{edge}})/k_B T]$. The model has seven parameters, here we report results for $\nu_0 = 10^{13} \text{ s}^{-1}$, $E_S = 1.5 \text{ eV}$, $E_N^T = 0.3 \text{ eV}$, $E_N^X = 0.1 \text{ eV}$, $E_A = 2.3 \text{ eV}$, $E_{\text{edge}} = E_{\text{diff}} = 0.35 \text{ eV}$, which gave the best agreement with experimental results. Using the model, we tried to reproduce both growth and equilibration processes on the Si/Si(111)7×7 surface on a real time- and spatial scale. The HUC in the model is thus considered to be 1 bilayer (BL) of Si(111) thick, of a triangular shape with the edge length of $a = 26.9 \text{ \AA}$ and consisting of 49 Si atoms. All calculations were performed on 200×200 HUC lattice with periodic boundary conditions.

Growth. We tried to fit the exponent χ given by

$$N \approx F^\chi \quad (1)$$

where the dependence of the island density N on flux F at a constant temperature is measured.^{1,2,5} The experimental value of $\chi = 0.75$ for $T = 680 \text{ K}$ and $T = 770 \text{ K}$ was reported in Ref. 13. In this experiment, samples were prepared at a given temperature by deposition of ≈ 0.15 BL Si on the Si(111)7×7 surface followed by rapid quenching to room temperature. The experimental morphologies of the layer can therefore be considered snapshots from the Si/Si(111)7×7 surface morphology evolution.

In the model, we calculated the flux dependence of the density of *transformed* (i.e., crystalline) islands N at constant *total* coverage Θ_{tot} (Ref. 14). Results are shown in Fig. 1. At lower fluxes, a power-law $N = F^\chi$ dependence with $\chi_{680} = 0.76 \pm 0.03$, $\chi_{770} = 0.75 \pm 0.04$ is observed. In the experiment, disordered growth occurred at high fluxes. In the model, deviations from the power-law behavior of $N = N(F)$ are observed.

The presence of the barriers to attachment in the model introduces specific features into its dynamical behavior. In the dependence of N on the total coverage Θ_{tot} (Fig. 2a) the nucleation onset (fast increase of N) takes place at higher coverages than in standard (minimal) growth model (Fig. 2b), Ref. 15. The maxima of $N(\Theta_{\text{tot}})$ are sharp and occur at higher Θ_{tot} than the broad maxima of the standard model.

Island growth in our model starts by a transformation of 3 neighboring HUCs.⁴ Due to the barriers to attachment this happens only after a certain time elapsed from HUC clustering. This time does *not* scale with flux in contrast to the time for clustering of units of material. Transformation becomes the rate-limiting process of island formation. By the time the transformation begins, more material has been deposited for the case of higher flux F . This shifts the nucleation onset and $N_{\text{max}}(\Theta_{\text{tot}})$ position to higher Θ_{tot} . With increasing F , amount of non-transformed material at a given Θ_{tot} increases (Fig. 2c), and so does the disorder of the quenched sample.

A newborn island composed of 3 units can further grow or decay. The competition between growth and decay of transformed clusters results in a steep decrease of $N(\Theta_{\text{tot}})$ for $N > N_{\text{max}}$. This decrease is *not* due to coalescence, because the islands at $N = N_{\text{max}}$ are small. Both the delay in island formation and the instability of islands leave traces in the time evolution of the mean island size, cf. Fig. 3.

The shift of N_{max} to higher Θ_{tot} than in standard model and the fast decrease of $N(\Theta_{\text{tot}})$ after reaching N_{max} contribute to the high value of χ observed at $\Theta_{\text{tot}} = \text{const}$ during growth with barriers to attachment. With the barrier to attachment decreasing and the nearest-neighbor bond strength increasing, χ decreases.

Analytical theories usually relate the value of the growth exponent χ to i^* , the number of material units in a “critical” (i.e., largest unstable) island in the growth system. For the determination of i^* , we can use a formula $\chi = 2i^*/(i^* + 3)$ derived by Kandel.^{5,16} χ in the model varies smoothly with E_S , E_N^X , and E_N^T so that the corresponding values of i^* are non-integer numbers between $i^* = 1$ ($\chi = 0.5$) and $i^* = 2$ ($\chi = 0.8$). In addition, a dependence of the island density on E_S (the substrate contribution to the hopping barrier) was found, in contrast to predictions of Ref. 6.

The instability of growing islands does not strongly affect morphologies obtained for Si/Si(111)7×7 MBE growth. We observe the characteristic multiple-peaked island size distribution (Fig. 4c, d), but with broader peaks (in better agreement with the experimental results) as compared to the model with detachment of material from islands forbidden.⁷ In the morphologies of experimental samples, non-transformed clusters of Si adatoms formed during quenching of samples are visible (Fig. 4b). The density of non-transformed material may be experimentally determined and compared to the model results.

Equilibration. The decay of Si/Si(111)7×7 reconstructed 1 BL-high adatom (A) and vacancy (V) islands was experimentally studied in Refs. 17–19. Using STM at an elevated temperature, the authors of Refs. 17 and 18 followed a number of isolated (a nearest island or a step edge at a distance more than 800 Å) adatom or vacancy islands and studied the temperature dependence of their decay rates. The decay rates ν^A , ν^V showed Arrhenius behavior $\nu^{A,V} = \nu_0^{A,V} \exp(-E_a^{A,V}/k_B T)$ with $\nu_0^A = 2 \times 10^{11 \pm 1} \text{ adatoms} \cdot \text{s}^{-1}$, $E_a^A = 1.5 \pm 0.1 \text{ eV}$ for

adatoms, $\nu_0^V = 3 \times 10^{9 \pm 1} \text{adatoms}\cdot\text{s}^{-1}$, $E_a^V = 1.3 \pm 0.2 \text{ eV}$ for vacancies, respectively. The decay rate of vacancy islands was found to be approx. 5 times lower than that of adatom islands.²⁰

With our model, we traced the evolution of a 96-HUC compact adatom or vacancy island placed on a vicinal Si surface (U-type steps, the terrace width of 480 nm, the distance from the descending step edge of 240 nm) equilibrated at a given temperature. Step edges on the vicinal surface form adatom sources and traps necessary for true disappearance of a single adatom or vacancy island in a model with periodic boundary conditions.

The temperature dependence of the decay rates for adatom and vacancy islands in our model is shown in Fig. 5a, b. With the parameters listed above, the decay rates in the model are higher than the experimental ones ($\nu_0^A = 3 \times 10^{14.5 \pm 0.5} \text{adatoms}\cdot\text{s}^{-1}$, $E_a^A = 2.1 \pm 0.1 \text{ eV}$, $\nu_0^V = 1 \times 10^{14 \pm 1} \text{adatoms}\cdot\text{s}^{-1}$, $E_a^V = 2.0 \pm 0.1 \text{ eV}$), and the decay rate of vacancy islands is approx. 2 times lower than the decay rate of adatom islands.

The authors of Ref. 17,18 attributed the difference between the decay rates of adatom and vacancy islands to the effect of the Ehrlich-Schwoebel (step-edge) barrier in the Si/Si(111)7×7 system. We do not believe that the Ehrlich-Schwoebel barrier plays any role: Growth experiments provide no compelling evidence of the presence of an appreciable Ehrlich-Schwoebel barrier at step edges on Si/Si(111)7×7 surface within the relevant temperature range.¹⁰

We also modeled adatom and vacancy islands decay with the barrier to attachment “switched off”.¹⁵ The decay rates thus obtained were lower ($\nu_0^A = 5 \times 10^{13 \pm 1} \text{adatoms}\cdot\text{s}^{-1}$, $E_a^A = 2.1 \pm 0.2 \text{ eV}$, $\nu_0^V = 1 \times 10^{12 \pm 1} \text{adatoms}\cdot\text{s}^{-1}$, $E_a^V = 2.1 \pm 0.2 \text{ eV}$), but the decay rate of vacancy islands was still approx. 2 times lower than for adatom islands. This observation agrees with results of a standard growth model on square lattice.²¹ The difference in these decay rates on the vicinal surface thus seems to originate from the difference of geometry of adatom and vacancy island boundaries.²¹

In Fig. 5c, a typical time evolution of the size of a decaying island in a model with the barriers to attachment is shown. We see that stable (“magic”) Si islands do exist. They correspond to equilibrium island shapes experimentally observed^{17–19} and differ from magic shapes observed during Si/Si(111)7×7 growth.⁷ Magic islands are compact (2 nearest-neighbors for all perimeter HUCs) and the barrier to attachment prevents their shape from “being spoiled” by attachment of material surrounding the island. No stable shapes are observed during island decay for the model without barriers to attachment.

In this work, we presented a coarse-grained model of Si/Si(111)7×7 MBE growth with an activation barrier to attachment of new material to existing islands implemented. We demonstrated that this barrier contributes to the steep growth-rate dependence of the island density observed in Si/Si(111)7×7 MBE and helps to stabilize “magic” island shapes in both growth and relaxation experiments.

This work was supported by the Grant Agency of the Czech Republic, project GAČR 202/97/1109.

* To whom correspondence should be addressed; e-mail: myslivec@plasma.troja.mff.cuni.cz.

¹ J. A. Venables, G. D. T. Spiller, M. Hanbücken, Rep. Prog. Phys. **47**, 399 (1984).

² C. Ratsch, A. Zangwill, P. Šmilauer, and D. D. Vvedensky, Phys. Rev. Lett. **72**, 3194 (1994); Surf. Sci. Lett. **329**, L599 (1995).

³ P.A. Mulheran and J.A. Blackman, Philos. Mag. Lett. **72**, 55 (1995); M.C. Bartelt and J.W. Evans, Phys. Rev. B **54**, R17359 (1996).

⁴ H. Tochihara and W. Shimada, Surf. Sci. **296**, 186 (1993).

⁵ D. Kandel, Phys. Rev. Lett. **78**, 499 (1997).

⁶ F. Thibaudau, Surf. Sci. Lett. **416**, L1118 (1998).

⁷ B. Voigtländer, M. Kästner, and P. Šmilauer, Phys. Rev. Lett. **81**, 858 (1998).

⁸ B. Voigtländer and T. Weber, Phys. Rev. B **54**, 7709 (1996).

⁹ B. Voigtländer and T. Weber, Phys. Rev. Lett. **77**, 3861 (1996).

¹⁰ B. Voigtländer, A. Zinner, T. Weber, and H. P. Bonzel, Phys. Rev. B **51**, 7583 (1995).

¹¹ K. Takayanagi, Y. Tanishiro, M. Takahashi, S. Takahashi, J. Vac. Sci. Technol. A **3**, 1502 (1985).

¹² “In vivo” record of Si/Si(111)7×7 MBE is presented at <http://www.fz-juelich.de/video/voigtländer/>.

¹³ L. Andersohn, Th. Berke, U. Köhler, and B. Voigtländer, J. Vac. Sci. Technol. A **14**, 312 (1996).

¹⁴ The exponent χ depends on the way N in Eq. (1) is determined. For our model, both N at constant *transformed* coverage Θ_{trans} and $N=N_{\text{max}}(\Theta_{\text{tot}})$ give a systematically lower χ .

¹⁵ A result obtained using our model with a zero barrier to transformation is presented.

¹⁶ Model parameters satisfy conditions for χ to follow the $\chi = 2i^*/(i^* + 3)$ (Ref. 5) dependence rather than the standard one, $\chi = i^*/(i^* + 2)$, Refs. 1,2.

¹⁷ A. Ichimiya, Y. Tanaka, and K. Ishiyama, Phys. Rev. Lett. **76**, 4721 (1996).

¹⁸ A. Ichimiya, Y. Tanaka, and K. Hayashi, Surf. Sci. **386**, 182 (1997).

¹⁹ U. Köhler, L. Andersohn, and B. Dahlheimer, Appl. Phys. A **57**, 491 (1993).

²⁰ The difference in the adatom and vacancy island decay rates¹⁸ resulted from a correction of raw data for STM tip effects. Without this correction, the decay rates were equal within the experimental error: $\nu_0^A = 2 \times 10^{10 \pm 1} \text{adatoms}\cdot\text{s}^{-1}$, $E_a^A = 1.3 \pm 0.1 \text{ eV}$, $\nu_0^V = 4 \times 10^{9 \pm 1} \text{adatoms}\cdot\text{s}^{-1}$, $E_a^V = 1.2 \pm 0.2 \text{ eV}$.

²¹ A. Natori, M. Murayama, D. Matsumoto, H. Yasunaga, Surf. Sci. **409**, 160 (1998).

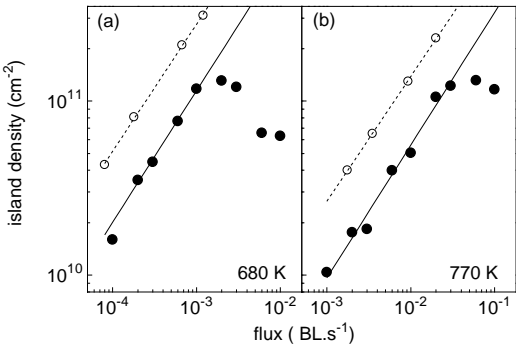


FIG. 1. Flux dependence of the island density N for Si/Si(111)7×7 MBE is $N=F^\chi$ with $\chi=0.75$. Experimental (○) (Ref. 13) and modeled (●) $N(F)$ dependencies for 680 K (a) and 770 K (b) are shown. In the model, N at $\Theta_{\text{tot}}=0.15$ BL was measured.

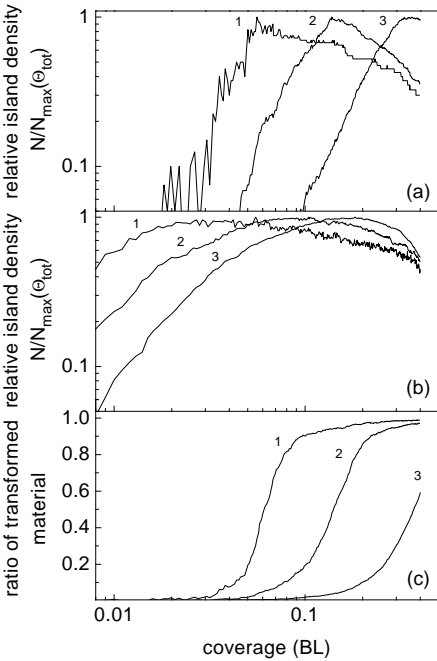


FIG. 2. Evolution of the island density vs. total coverage for a model with the barriers to attachment depends on flux (a) and differs from that of a standard growth model (b), Ref. 15. The barrier to attachment limits the rate of creation of reconstructed islands. At high fluxes, most of the material present at the surface is non-transformed (c). Data for (1) $F=10^{-4}$ BL·s⁻¹, (2) $F=10^{-3}$ BL·s⁻¹, and (3) $F=10^{-2}$ BL·s⁻¹ are shown.

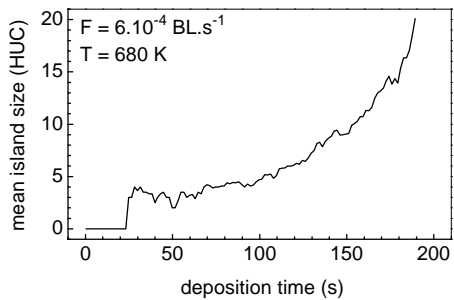


FIG. 3. The delay of island creation is clearly visible in the record of the mean island size time evolution. Instability of newborn islands causes the decrease of $\langle s \rangle$ at short times.

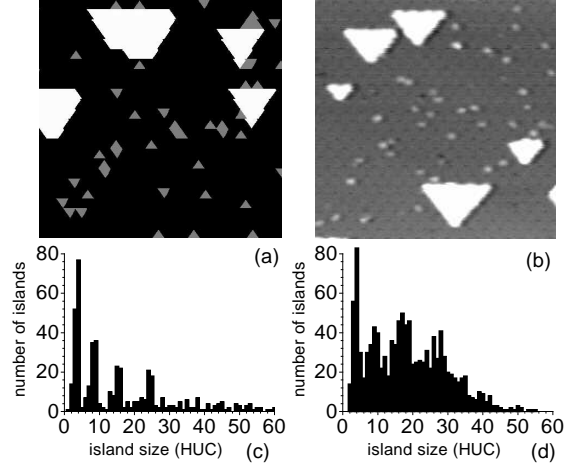


FIG. 4. Growth morphologies in the model (a) and experiment (b). During growth, magic island sizes are stabilized, resulting in a non-trivial island size distribution (c, d), Ref. 7.

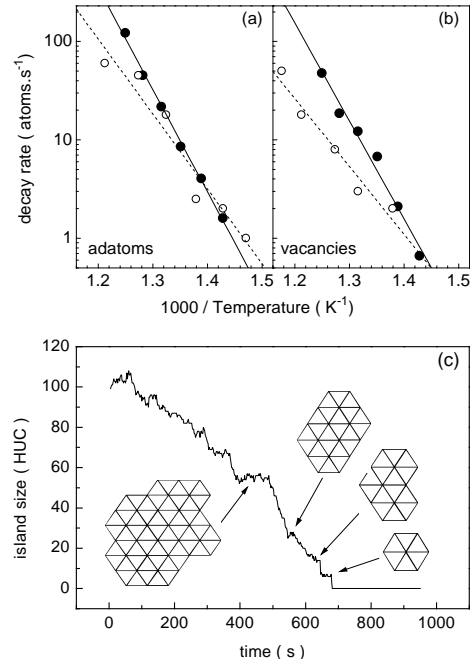


FIG. 5. Arrhenius plots of experimental (○) (Ref. 17) and modeled (●) decay rates for adatom (a) and vacancy (b) islands. In the model, the rate of vacancy filling is 2× lower than that of adatom islands decay. During island decay, “magic” island sizes are stabilized (c). Insets show some of the observed stable island morphologies. These are close to equilibrium island shapes^{17–19} and differ from “magic” island shapes observed during growth (cf. Fig 4b).